

## Superlattice Dislocations on {111} and {001} in Superalloys

A. Huis in't Veld, G. Boom, P. M. Bronsveld, J. Th. M. De Hosson

Department of Applied Physics, Materials Science Centre  
University of Groningen, Nijenborgh 18, 9747 AG Groningen  
The Netherlands

(Received November 2, 1984)

Introduction

Ni-base superalloys for high temperature applications are well known for their resistance to creep (1). This is due to a uniform array of  $\gamma'$  precipitates which resist overall deformation of the material. Unfortunately, at very high temperatures ( $> 1270$  K), these  $L1_2$  ordered  $Ni_3Al$  particles coarsen and eventually redissolve to form a relatively weak structure. Consequently, fine particles of oxides, having many times the stability of  $\gamma'$ -particles at high temperatures, are usually added in order to improve the creep resistance. This paper reports on the interaction between dislocations and  $\gamma'$ -precipitates at 1003 K. At this temperature the  $\gamma'$  particles are still strong obstacles for moving dislocations.

Besides the engineering interest in these superalloys containing  $L1_2$  ordered precipitates (1), a great deal of scientific interest has been shown in the mechanical behaviour of  $L1_2$  ordered alloys. Recently, Veyssi re, Guan and Rabier (2) concluded from weak beam observations of dislocations in polycrystalline ordered  $Ni_3Al$  that climb has played a substantial role. Temperature strengthening due to climb dissociation may play an important role in the interpretation of the strong temperature dependence of the yield and flow stresses of  $L1_2$  ordered alloys. So far, based on experiments, two different models have been proposed to explain this anomalous behaviour: a dynamic interaction between dislocations on {111} planes and sessile segments which have cross-slipped onto {001} due to thermal activation (3)(4).

Chou, Hirsch, McLean and Hondros (5) observed antiphase domain boundary tubes in polycrystalline  $Ni_3Al$  which may be a contributor to the high strength of this alloy, although it is not clear whether the peak in the curve of flow stress as a function of temperature may be associated with the temperature at which climb helps jogs in a dislocation to align.

In the present work we focused on characteristic features of dislocations in  $\gamma'$  precipitation strengthened nickel-base superalloys; in particular whether {001} climb dissociation in precipitation strengthened material could be observed.

With respect to dislocation reactions in Ni-base superalloys containing  $L1_2$  ordered precipitates, cutting of  $\gamma'$  precipitates by pairs of  $1/2 \langle 110 \rangle$  superlattice dislocations on {111} planes are expected. Glide of a unit dislocation in an f.c.c. superlattice results in the production of an antiphase boundary in its wake. A second dislocation, having the same Burgers vector, gliding in the same slipplane, will cancel the APB produced by the first dislocation. Hence, it is energetically more favourable for the  $L1_2$  lattice to deform by the glide of a pair of unit dislocations, which minimizes the energy of disorder by confining the APB. From the separation of the unit dislocations the energy of the APB can be determined experimentally. The APB energy on {111} can be written as:

$$E_{\{111\}}^{APB} = \frac{-2 w^{(1)}}{\sqrt{3} a_0^2}, \quad (1)$$

where  $w^{(1)}$  is the effective ordering energy at the first nearest neighbour and  $a_0$  represents the lattice parameter. In contrast, no contributions to the energy of the APB on {001} come from the first-neighbour interactions, as first noted by Flinn (6):

$$E_{\{100\}}^{\text{APB}} = \frac{+2 W^{(2)}}{a_0^2}, \quad (2)$$

where  $W^{(2)}$  is the ordering energy at the second nearest neighbour.

From eqs. (1)(2), it can be concluded that TEM observations of the separations of superlattice dislocations both on  $\{111\}$  and on  $\{100\}$  may provide experimental information about the ratio  $W^{(2)}/W^{(1)}$ .

In particular, experimental values of  $W^{(2)}/W^{(1)}$  are important for predicting phase diagrams and the ground state structures in ordered alloys. In the case of f.c.c. and b.c.c. lattices, the ground states have been predicted several years ago using first and second neighbour interactions (7)(8). More complicated structures have been handled by Sanchez and DeFontaine (9). For example when  $W^{(1)} < 0$  and  $W^{(2)}/W^{(1)} < 0$   $L1_2$  is predicted the ground state for A<sub>3</sub>B. In the range  $0 < W^{(2)}/W^{(1)} < 1/2$ , however,  $D0_{22}$  is predicted to be ground state. Despite the large amount of research done on the theoretical side, scant experimental information is available about  $W^{(2)}/W^{(1)}$ .

### Experimental Procedure

The material employed for this study was the precipitation hardened nickel-base Astroloy. The test specimens fractured after about 100 fatigue cycles at 1003 K with  $\dot{\epsilon} = 5 \times 10^{-3} \text{ s}^{-1}$  and  $\Delta\epsilon = 3 \times 10^{-4}$  (10). The chemical composition of powder metallurgical (PM) Astroloy is given in Table 1.

TABLE 1

The chemical composition of PM Astroloy

Elements	Ni	Co	Cr	Mo	Al	Ti	C	B
wt%	bal	16.62	14.92	4.95	3.70	3.54	0.02	0.02

Analysis gives evidence for Fe, Mn, Si, S, O<sub>2</sub>, Cu and N to be present in PM Astroloy in a small amount. The matrix of Astroloy is hardened by 48 volume %  $\gamma'$  precipitates which can be grouped into three categories as far as their sizes are concerned. Cuboids with edge lengths of 100-200 nm and small spherical particles (diameter 50-60 nm) between the cuboids. Cuboids with edge lengths of 1-4  $\mu\text{m}$  are found along the grain boundaries and groups of eight in the matrix. After LCF testing at 1003 K with  $\dot{\epsilon} = 10^{-2} \text{ s}^{-1}$  the planar character of slip is illustrated by sheared precipitates (fig.1). The sheared distance indicates the passage of about 150 unit dislocations.



Fig. 1

SEM picture of cuboids (100-200 nm) and spheres (50-60 nm), one of the cuboids is sheared.

After fracture the smooth surface was cleaned electrochemically (about 10 V) with the etchant in an ultrasonic cleaning apparatus. The cleaning procedure was followed by etching for about 10 sec with the same etchant: 85% acetic acid, 10% perchloric acid and 5% water.

Disk type specimens for TEM observations were obtained from the tested material by spark cutting to minimize deformation. The samples were electrochemically thinned in a polishing equipment at room temperature. The thinned specimens were examined in a JEM 200 CX electron microscope with a selected area magnification of 100 K.

### TEM Observations

Superlattice dislocations were imaged in dark-field using the weak beam technique (11). Identification of the slip plane is performed using stereo microscopy. The Burgers vector of the dislocation has been determined using the criterion that a dislocation is invisible if  $\mathbf{g} \cdot \mathbf{b} = 0$  and  $\mathbf{g} \cdot (\mathbf{b} \times \mathbf{u})$  is sufficiently small ( $\lesssim 0.5$ ), where  $\mathbf{g}$  is the diffraction vector,  $\mathbf{b}$  is the Burgers vector and  $\mathbf{u}$  represents the unit vector along the dislocation line.

A typical example of a superlattice dislocation pair with a Burgers vector  $\mathbf{b} = \frac{1}{2} a_0 [\bar{1}01]$  is depicted in fig. 2. It has to be emphasized that the dislocation pair presented here is just an example out of a large number of similar zigzag shaped dislocations. Two micrographs with  $\mathbf{g} = [\bar{2}00]$  forming a stereo set were used to construct a three-dimensional image. The deviation from the Bragg position, characterized by  $w$ , was chosen to be 8.7. This value causes a narrow image of the dislocation and hence reveal more detail. But the larger  $w$  the smaller the intensity of the image and the longer will be the exposure time necessary to image the dislocation on an electron micrograph. Long exposure times require a high stability of the electron microscope. Hence, there is an optimum in operating the electron microscope to reveal as much detail as possible, using the weak-beam technique. To determine the value for  $w = s_g \xi$  one needs first to calculate the extinction distance  $\xi_{200}$ .



Fig. 2

Stereo TEM image of a superlattice dislocation using a stereo angle of  $32.4^\circ$ .

The beam direction is between  $[0\bar{1}1]$  and  $[001]$ , the stereo axis is  $\mathbf{g} = [\bar{2}00]$  while  $w = 8.7$ .

In this article we have based our calculations on a  $L1_2$  unit cell with Ni and Co statistically distributed over three sublattices and Al and Ti distributed statistically over the remaining sublattice. In such a way we found for the extinction distance  $\xi_{200} = 42$  nm using the manufacturer's data for the concentrations. The stereo set can best be interpreted by assuming a glissile part on  $(\bar{1}\bar{1}1)$  a cross-slipped part on  $(001)$  oriented along  $[010]$  and a part which has climbed towards  $(\bar{1}\bar{1}1)$ . These three main sections are indicated separately on fig. 3.

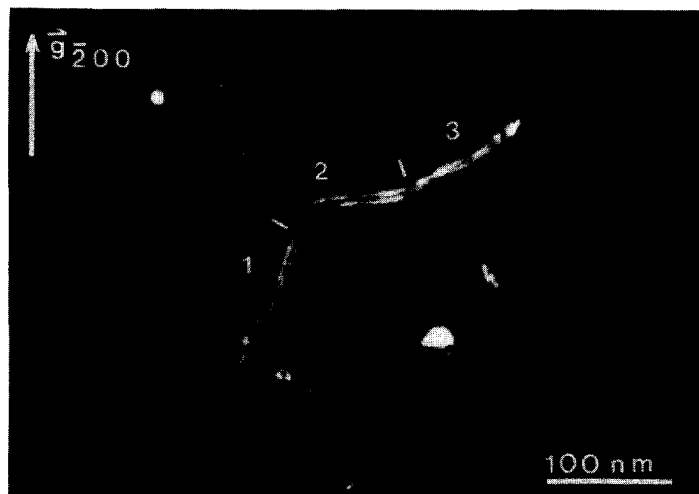


Fig. 3

Three main sections of the superlattice dislocation: 1: screw part on  $(1\bar{1}1)_L$ , 2: cross-slipped part on  $(001)$ , 3: double cross-slipped part climbed towards  $(1\bar{1}1)$ .

The reaction is that of a double cross-slip mechanism although the cause of the cross-slip could not be pinpointed. As a matter of fact the  $\gamma'$  precipitates could not be visualized at all due to heavy deformation. Hardly any intensity was left on the superlattice 100 and 110 spots. The dissociation distance of the superlattice dislocation would change abruptly if part of the dislocation was located outside a  $\gamma'$  precipitate. (The trailing one would be attracted resulting in a narrow dissociation.) Therefore, we assume the whole configuration inside a  $\gamma'$  precipitate. It is physically plausible that the dislocation configuration is strongly influenced by the process of entering a  $\gamma'$  precipitate. Nevertheless, the distance  $d$  measured between the dislocations on  $(1\bar{1}1)$  determined from fig. 4 is 3.5 nm.

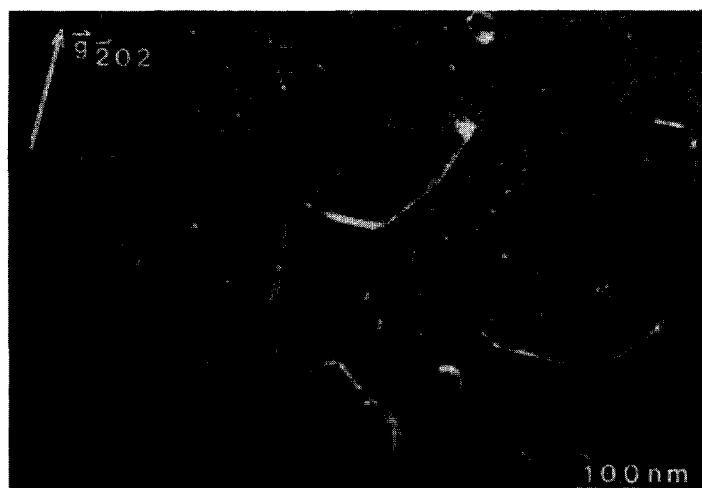


Fig. 4

Dissociation of the screw part on  $(1\bar{1}1)$ . The Burgers vector  $\mathbf{b} = a_0/2 [101]$  and  $w = 15$ .

The APB energy for a mixed superlattice dislocation is given by the following equation:

$$E^{\text{APB}} = \frac{b^2 \mu}{2\pi d} \left( \cos^2 \theta + \frac{\sin^2 \theta}{1-\nu} \right), \quad (3)$$

where  $d$  represents the equilibrium separation,  $\mu$  is the shear modulus (66.61 GPa),  $\nu$  is Poisson's ratio (0.3) and  $\theta$  is the angle between the dislocation line and the Burgers vector  $b$  (0.25 nm). Using the experimental value for the superlattice dislocation separation of the screw parts ( $d=3.5$  nm) in eq. (3), the APB energy on {111} is calculated to be 189 mJ/m<sup>2</sup>. For the parts in edge orientation on {001}, a dissociation of 9.1 nm at maximum (fig. 2) is found leading to an APB energy on {001} of 104 mJ/m<sup>2</sup>, which is in reasonable agreement with the recently reported value by Veyssi re on polycrystalline Ni<sub>3</sub>Al (140 ± 14 mJ/m<sup>2</sup>) (14). It should be emphasized that these are extreme values since internal stresses might change the values obtained for the APB energies considerably. Although the separations of the superlattice dislocations may be affected by these stresses, the influence is assumed to be smaller when the ratio of the APB energies on {111} and {001} is considered:

$$\frac{E_{\{001\}}}{E_{\{111\}}} = - \frac{W^{(2)}}{W^{(1)}} = -0.32.$$

This ratio and the experimental findings that  $W^{(1)} < 0$  and  $W^{(2)} > 0$  predict a stable L1<sub>2</sub> structure. From the absolute value of the APB energy on {111} a critical temperature for L1<sub>2</sub> ordering of 1414 K is predicted in terms of an *effective* ordering energy, according to (12):

$$T_c = 0.96225 \frac{W^{(1)}}{k}, \quad (4)$$

in reasonable agreement with experimental observations (13).

The photographs suggest that a continuous transition from (111) to (001) occurs. Our findings in precipitation strengthened material are analogous to the experimental results obtained by Veyssi re et al. (2) (14) in polycrystalline Ni<sub>3</sub>Al as far as the climb process towards {001} is concerned. It is not clear yet whether this temperature strengthening process due to climb dissociation plays an important role in the mechanical behaviour of the superalloys under investigation.

### Conclusions

Characteristic features of dislocations in  $\gamma'$  precipitation strengthened nickel-base superalloys were studied in dark-field using the weak-beam technique. Stereo-measurements of the images proved to be an effective tool for determining the three dimensional configuration of superlattice dislocations. We have focussed on superlattice dislocations present in Ni-base superalloys fractured after about 100 fatigue cycles at 1003 K with strain rate of 5 10<sup>-5</sup> s<sup>-1</sup> and amplitude  $\Delta\epsilon = 3 \cdot 10^{-4}$ . In addition to {111} cross slip behaviour, temperature strengthening due to climb dissociation onto {001} has been observed.

From TEM observations the dissociation width of superlattice dislocations has been measured on both {111} and {001}. These two widths have been used to calculate the ratio of the APB energy on {111} and {001} leading to a ratio of the ordering energies of the first and second neighbouring interaction  $W^{(2)}/W^{(1)}$  being -0.32, in accordance with theoretical predictions of the L1<sub>2</sub> ground state.

### References

1. T. E. Howson, D. A. Mervyn, J. K. Tien, Met. Trans. **11A**, 1609 (1980) (and ref. therein).
2. P. Veyssi re, D. L. Guan and J. Rabier, Phil. Mag. **49**, 45 (1984).
3. S. Takeuchi and E. Kuramoto, Acta Metall. **21**, 415 (1973).
4. S. J. Liang and D. P. Pope, Acta Metall. **25**, 485 (1977).
5. C. T. Chou, P. B. Hirsch, M. McLean and E. Hondros, Nature **300**, 621 (1982).
6. P. A. Flinn, Trans. Am. Inst. Min. Engrs. **218**, 145 (1960).
7. J. Kanamori, Progr. Theor. Phys. **35**, 16 (1966).

8. S. M. Allen, J. W. Cahn, *Acta Metall.* **20**, 423 (1972).
9. J. M. Sanchez, D. De Fontaine, in: *Structure and Bonding in Crystals*, M. O'Keefe and A. Navrotsky, eds., Acad. Press, N.Y., (1981) p. 117.
10. J. Bressers, M. Roth, ASME Conference on Life Time Prediction, Albany, USA, 18-20 April, 1982.
11. D. J. H. Cockayne, *Z. f. Naturforschung* **27a**, 452 (1972).
12. D. De Fontaine, in: *Solid State Physics*, H. E. Ehrenreich, F. Seitz, D. Trunbull, eds., Vol. **34** (1979).
13. M. Hansen, *Constitution of Binary Alloys*, Mc Graw Hill, N. Y. 1958.
14. P. Veyssi re, *Phil. Mag.* **50**, 189 (1984).